AGU PUBLICATIONS

JGR

Journal of Geophysical Research: Atmospheres

RESEARCH ARTICLE
10.1002/2017JD027418

Trends and Variability of Surface Solar Radiation in Europe Based On Surface- and Satellite-Based Data Records

Uwe Pfeifroth[1], Arturo Sanchez-Lorenzo[2,3], Veronica Manara[4], Jörg Trentmann[1], and Rainer Hollmann[1]

[1]Satellite-Based Climate Monitoring, Deutscher Wetterdienst, Offenbach, Germany, [2]Pyrenean Institute of Ecology, Spanish National Research Council (CSIC), Zaragoza, Spain, [3]Department of Physics, University of Extremadura, Badajoz, Spain, [4]Now at Institute of Atmospheric Sciences and Climate, ISAC-CNR, Bologna, Italy

Key Points:
- CMSAF's satellite climate data record of surface solar radiation have high accuracy and stability
- Surface solar radiation trends given by the satellite data and the station data agree well for Europe, except for the Mediterranean summer
- The main reason for the observed trends of surface solar radiation in Europe is changes in clouds

Correspondence to:
U. Pfeifroth,
uwe.pfeifroth@dwd.de

Citation:
Pfeifroth, U., Sanchez-Lorenzo, A., Manara, V., Trentmann, J., & Hollmann R. (2018). Trends and variability of surface solar radiation in Europe based on surface- and satellite-based data records. *Journal of Geophysical Research: Atmospheres*, *123*, 1735–1754. https://doi.org/10.1002/2017JD027418

Received 7 JUL 2017
Accepted 20 DEC 2017
Accepted article online 6 JAN 2018
Published online 7 FEB 2018

Abstract The incoming solar radiation is the essential climate variable that determines the Earth's energy cycle and climate. As long-term high-quality surface measurements of solar radiation are rare, satellite data are used to derive more information on its spatial pattern and its temporal variability. Recently, the EUMETSAT Satellite Application on Climate Monitoring (CM SAF) has published two satellite-based climate data records: Surface Solar Radiation Data Set-Heliosat, Edition 2 (SARAH-2), and Clouds and Radiation Data Set based on AVHRR (advanced very high resolution radiometer) Satellite Measurements, Edition 2 (CLARA-A2). Both data records provide estimates of surface solar radiation. In this study, these new climate data records are compared to surface measurements in Europe during the period 1983–2015. SARAH-2 and CLARA-A2 show a high accuracy compared to ground-based observations (mean absolute deviations of 6.9 and 7.3 W/m^2, respectively) highlighting a good agreement considering the temporal behavior and the spatial distribution. The results show an overall brightening period since the 1980s onward (comprised between 1.9 and 2.4 W/m^2/decade), with substantial decadal and spatial variability. The strongest brightening is found in eastern Europe in spring. An exception is found for northern and southern Europe, where the trends shown by the station data are not completely reproduced by satellite data, especially in summer in southern Europe. We conclude that the major part of the observed trends in surface solar radiation in Europe is caused by changes in clouds and that remaining differences between the satellite- and the station-based data might be connected to changes in the direct aerosol effect and in snow cover.

Plain Language Summary The incoming solar radiation is the essential climate variable that determines the Earth's climate. As surface measurements of solar radiation are rare, satellite data are used to derive more information in space and time. Recently, the EUMETSAT Satellite Application on Climate Monitoring (CM SAF) has published two new satellite-based climate data records: Surface Solar Radiation Data Set-Heliosat, Edition 2 (SARAH-2), and Clouds and Radiation Data Set based on AVHRR (advanced very high resolution radiometer) Satellite Measurements, Edition 2 (CLARA-A2). Both satellite-based data records provide estimates of surface solar radiation and can capture what is observed by station measurements in Europe. The proven high accuracy of the CM SAF's climate data records allows the detailed analysis of surface solar radiation during the last three decades. A positive trend is observed by the station and satellite data, meaning surface radiation has increased since the 1980s, mainly in eastern and northwestern Europe. Some discrepancies between satellite and station data are found in the Mediterranean summer likely due to aerosol effects. It is concluded that the main reason for the observed positive trend in surface solar radiation in Europe since the 1980s is a change in clouds.

1. Introduction

Solar radiation is an essential climate variable and the main energy source for the Earth-atmosphere system (Ohmura & Gilgen, 1993; Ramanathan et al., 2001; Wild et al., 2015). High-quality and long-term measurements of the solar radiation are of major importance for our understanding of the climate system (Hartmann et al., 1986). Further, surface solar radiation (SSR) is a main constitute for the surface radiation budget (Wild et al., 2017) that, for example, determines the temperatures of the troposphere. Moreover, the SSR is of high importance not only for climate studies but also for many other applications, for example, solar energy production

(Huld et al., 2017; Miglietta et al., 2017; Wild et al., 2015), agriculture (Stanhill & Cohen, 2001), and vegetation dynamics (e.g., Mercado et al., 2009).

Available studies document a widespread reduction (3–9 W/m^2) of SSR from the 1950s to the 1980s called "global dimming" (Stanhill & Cohen, 2001) and a subsequent increase (1–4 W/m^2) since the 1980s called "brightening" (Gilgen et al., 2009; Wild et al., 2005; Wild, 2009). These variations are mostly due to changes in the transparency of the atmosphere due to variations in cloudiness and/or changes in anthropogenic aerosol emissions (Liepert et al., 1994; Stanhill & Cohen, 2001; Wild, 2009, 2016). However, the full understanding of the mechanisms and the contributions of both phenomena to the observed changes are still uncertain due to, for example, the lack of long-term SSR data, especially over ocean, remote land areas (e.g., Africa and Siberia), and areas characterized by complex orography (e.g., the Alpine region) (Sanchez-Lorenzo et al., 2015; Wild, 2009, 2012). Here data from satellite observations (e.g., those provided by the EUMETSAT Satellite Application Facility on Climate Monitoring-CM SAF) provide valuable additional information (Schulz et al., 2009), as they deliver an unique spatial coverage since the 1980s for both land and oceans (Hinkelmann et al., 2009; Karlsson et al., 2017b; Raschke et al., 2016; Zhang et al., 2015).

The highest quality of ground-based measurements of SSR is collected in the Baseline Surface Radiation Network (BSRN) Archive (Ohmura et al., 1998). Unfortunately, globally, there are only about 50 BSRN stations available and their temporal coverage starts in 1992. Therefore, BSRN cannot be used to evaluate variability and trends given by the satellite records on climatological scale. For Europe, several long-term station measurements are available and have been used already for the analysis of trends and changes, the Global Energy Budget Archive (GEBA) (Sanchez-Lorenzo et al., 2017; Wild et al., 2017), the World Radiation Data Center (WRDC), and measurements provided and managed by individual countries (e.g., Manara et al., 2016; Sanchez-Lorenzo et al., 2013).

Satellite-based data of SSR from the CM SAF have been validated by Urraca et al. (2017) in Europe using station measurements from national and international databases. It was found that the CM SAF satellite-based SSR data are of a high quality. Sanchez-Lorenzo et al. (2017) used European station data and a former version of the CM SAF satellite data of SSR to validate trends in Europe during the time period 1983–2010. They found overall positive trends of SSR in Europe and largest trends in spring.

In this study, two satellite-based climate data records of SSR provided by the CM SAF are evaluated with surface measurement in Europe for the time period 1983–2015 to assess their accuracy and their ability to capture temporal and spatial variability of SSR in Europe. The data and methods used in this study are presented in sections 2 and 3, respectively. A basic evaluation is shown in section 4, and the trend and variability analysis is shown in section 5. The discussion of results and conclusions are presented in section 6.

2. Data

The data used in this study are two climate data records generated by the CM SAF, namely, the Surface Solar Radiation Data Set-Heliosat, Edition 2 (SARAH-2), and the CM SAF Clouds, Albedo and Radiation Data Set from advanced very high resolution radiometer (AVHRR) data, Edition 2 (CLARA-A2). For validation purposes ground-based SSR measurements are used.

2.1. Station Data

Long-term measurements of SSR are freely available from the Global Energy Budget Archive (GEBA) (Sanchez-Lorenzo et al., 2015; Wild et al., 2017), maintained by the ETH in Zurich, Switzerland, and from the World Radiation Data Center (WRDC) in St. Petersburg, Russia (http://wrdc.mgo.rssi.ru/). Even though all station data have been subject to a quality control and homogenization procedure, the data used in this study have been additionally checked. Additional measurements from Spain (Sanchez-Lorenzo et al., 2013) and Italy (Manara et al., 2016) are used in this study. Overall, 53 stations of monthly SSR measurements over Europe, providing data in the 1983–2015 period, have been collected. A list of all stations including further site information is shown in Table 1. Figure 1 shows the map of the analyzed area (Europe) including the station locations. The stations are relatively equally distributed (except the southeastern part of Europe) and cover different climate zones. The stations were further divided into five regions with similar temporal variability (determined by means of a principal component analysis, Sanchez-Lorenzo et al., 2015), as indicated in Figure 1. This regionalization of stations allows for a condensed and more robust regional trend analysis.

Table 1
List of the 53 Stations Used in This Study

Station	Longitude (°W)	Latitude (°N)	Country	Region
Aberdeen	−2.083	57.167	Great Britain	NW
Aberporth	−4.570	52.130	Great Britain	NW
Ajaccio	8.800	41.920	France	S
Albacete	−1.860	38.950	Spain	S
Aldergrove	−6.220	54.650	Great Britain	NW
Belsk	20.780	51.830	Poland	CE
Bergen	5.320	60.400	Norway	NW
Bratislava	17.100	48.170	Slovak Republic	CE
Caceres	−6.340	39.470	Spain	S
Cagliari	9.050	39.250	Italy	S
Clermont-Ferrand	3.167	45.783	France	CW
Clones	−7.233	54.183	Ireland	NW
Coruna	−8.380	43.300	Spain	CW
De Bilt	5.180	52.100	Netherlands	CE
De Kooy	4.783	52.917	Netherlands	CE
Dijon	5.083	47.267	France	CW
Dublin	−6.250	53.433	Ireland	NW
Dunstaffnage	−5.433	56.467	Great Britain	NW
Eelde	6.583	53.133	Netherlands	CE
Embrun	6.500	44.567	France	CW
Eskdalemuir	−3.200	55.320	Great Britain	NW
Helsinki	24.970	60.320	Finland	N
Hohenpeissenberg	11.020	47.800	Germany	CE
Hradec-Kralove	15.850	50.250	Czech Republic	CE
Jokioinen	23.500	60.820	Finland	N
Klagenfurt	14.330	46.650	Austria	CE
Lerwick	−1.180	60.130	Great Britain	NW
Logrono	−2.330	42.450	Spain	CW
Maastricht	5.783	50.917	Netherlands	CE
Madrid	−3.680	40.410	Spain	S
Malin-Head	−7.333	55.367	Ireland	NW
Millau	3.020	44.120	France	CW
Montpellier	3.967	43.583	France	CW
Murcia	−0.800	37.790	Spain	S
Nancy-Essey	6.220	48.680	France	CE
Nice	7.200	43.650	France	S
Odessa	30.630	46.480	Ukraine	CE
Oviedo	−5.870	43.350	Spain	CW
Palma de Mallorca	2.740	39.570	Spain	S
Perpignan	2.867	42.733	France	CW
Pisa	10.400	43.683	Italy	S
Potsdam	13.100	52.380	Germany	CE
Rennes	−1.733	48.067	France	CW
San Sebastian	−2.040	43.310	Spain	CW
Santander	−3.800	43.490	Spain	CW
Stockholm	17.950	59.350	Sweden	N
Strasbourg	7.633	48.550	France	CE

Table 1 *(continued)*

Station	Longitude (°W)	Latitude (°N)	Country	Region
Toravere	26.470	58.270	Estonia	N
Valentia	−10.250	51.930	Ireland	NW
Vigna di Valle	12.211	42.081	Italy	S
Vlissingen	3.600	51.450	Netherlands	CE
Warszawa	20.980	52.270	Poland	CE
Zakopane	19.970	49.280	Poland	CE

2.2. Clouds, Albedo and Radiation Data Set From AVHRR Data — Edition 2

The CM SAF Clouds, Albedo and Radiation data set from AVHRR data — Edition 2 (CLARA-A2, Karlsson et al., 2017a), covers the time period 1982–2015 and provides radiation and cloud parameters as daily and monthly means. The data record is based on the polar-orbiting satellite measurements from the advanced very high resolution radiometer (AVHRR) and is available globally with a spatial resolution of 0.25° × 0.25°. More information about the CLARA-A2 satellite retrieval and the available data records is provided by Karlsson et al. (2017b).

Beside various cloud information and the surface albedo, the CLARA-A2 climate data record contains upwelling and downwelling surface longwave radiation as well as SSR. The accuracy of monthly SSR from CLARA-A2 has been assessed by Karlsson et al. (2017b). It is found that the monthly mean CLARA-A2 SSR data have a small negative bias of −1.6 W/m^2 and a mean absolute bias of 8.8 W/m^2 with reference to globally distributed station data from BSRN.

A known deficiency influencing the quality of SSR in the CLARA-A2 climate data record is the availability of only a single AVHRR instrument at any given time during the first decade of the data record (1982–1991). Therefore, the spatiotemporal sampling of CLARA-A2 is limited during the early period, which leads to an increased number of missing data to estimate monthly means in the region of interest, reaching up to 50% missing data in southern Europe. From 1992 onward the spatiotemporal coverage is more complete. After 1992 the local overpass times of the used polar-orbiting satellites are in the morning and afternoon — at about

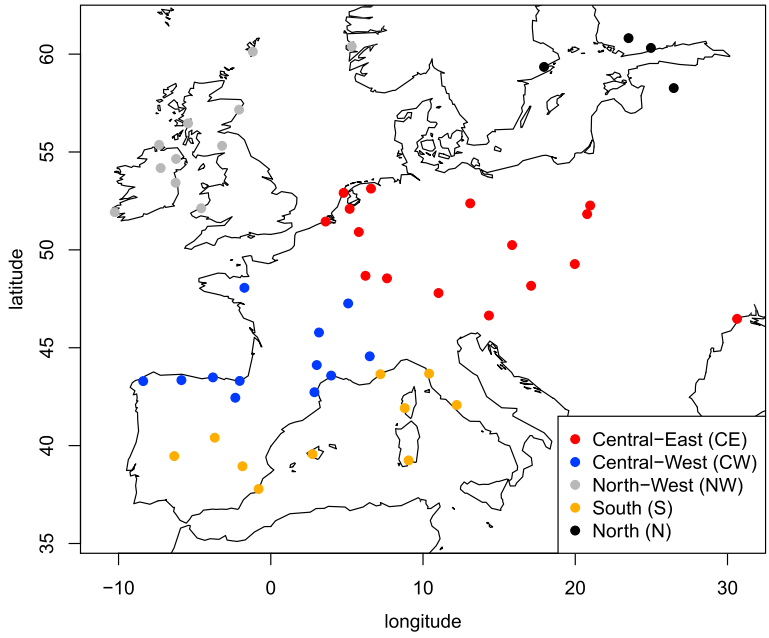

Figure 1. Stations used to evaluate satellite climate data records. The colors represent the corresponding regions as defined by a principal component analysis (red: central east, blue: central west, gray: northwest, orange: south, and black: north).

7.00 and 15.00 local time, respectively. Since 2002 a third satellite observes Europe at about 10.00 local time. Detailed information on the satellite orbits can be found in Figure 1 from Karlsson et al. (2017b).

2.3. Surface Solar Radiation Data Set-Heliosat, Edition 2

The Surface Solar Radiation Data Set-Heliosat, Edition 2 (SARAH-2, Pfeifroth et al., 2017), is the latest CM SAF climate data record of surface radiation based on the geostationary Meteosat satellite series covering Africa, Europe, and the Atlantic Ocean. It is the follow-up of the widely used SARAH climate data record (e.g., Müller, Pfeifroth, Traeger-Chatterjee, Trentmann, et al., 2015; Riihelä et al., 2015; Zăk et al., 2015). SARAH-2 covers the time period 1983–2015 and offers global and direct radiation parameters as well as the effective cloud albedo. SARAH-2 is provided as daily and monthly means and as half-hourly instantaneous data. Furthermore, sunshine duration and spectrally resolved radiation are available (Kothe et al., 2017). SARAH-2 covers the region of −65° to +65° in longitude and latitude and offers a high spatial resolution of 0.05° × 0.05°. A thorough overview of the basic retrieval principle of the SARAH climate data record series can be found in Müller, Pfeifroth, Traeger-Chatterjee, Trentmann, et al. (2015). SARAH-2 has been improved over the previous data record SARAH-1 especially by improving the stability in the early years and during the transition from the MVIRI (Meteosat Visible and Infrared Imager) to the SEVIRI (Spinning Enhanced Visible and Infrared Imager) instrument in 2006. Further, a correction to better account for slant viewing geometries has been applied and topographically corrected integrated water vapor data have been used.

The accuracy of the new SARAH-2 climate data record with reference to BSRN is documented in the CM SAF's Validation Report (Pfeifroth et al., 2017) available at http://www.cmsaf.eu/. A positive bias of +2 W/m^2 and an absolute bias of 5.1 W/m^2 for the monthly mean SARAH-2 SSR data have been found.

3. Methods

All data records are used as monthly means. For comparisons of the gridded satellite data with the station data, the satellite data are extracted at the station locations, by selecting the satellite pixel in which the station is located. The conducted trend calculations for the data records are based on linear regression analysis and based on monthly anomalies with reference to their long-term monthly means. Trends are analyzed at the spatial and at the seasonal scale, which provides new insights on the temporal and, in case of the satellite data records, also on the spatial variability. The seasons are defined as follows: winter (DJF: December–February), spring (MAM: March–May), summer (JJA: June–August), and autumn (SON: September–November). In case of spatially averaged trends, the anomalies derived for the individual station or satellite pixel time series are first averaged in space and then the trends are calculated as described above. The obtained trends for each data set are then presented either in the way of so-called Trendraster-plots or, in case of spatial trends, as spatial maps.

The Trendraster-plot, or running-trend analysis (Brunetti et al., 2006), is a way to represent, in a condensed way, the trends for different subperiods with different lengths. The advantage of the Trendraster-plots is that midterm and longer-term variability can be compared easily. Specifically, the *y* axis represents the starting year, while the *x* axis represents the last year of the considered period. The color of each pixel shows the intensity (linear trend W/m^2/decade) of the trend in the considered period.

In some cases 95% confidence intervals of the linear trends are given. These confidence intervals are used to analyze whether a trend is statistically significantly positive (negative), which is the case if both the lower and upper 95% confidence interval are positive (negative). Further, if the confidence intervals of trends derived from different data do overlap, they can be considered to be not statistically different.

4. Evaluation of Accuracy

In this section a basic validation of the CLARA-A2 and SARAH-2 climate data records with reference to the 53 stations in Europe is presented. A prerequisite for satellite climate data records be usable for climate purposes is to reasonably reproduce anomalies. Further, a low bias and low mean absolute deviations (MAD) compared to reference measurements are desired.

Figure 2 shows the mean SSR based on the two CM SAF climate data records analyzed in this study. Both data records overall agree in the general structure of SSR for Europe. For the CLARA-A2 climate data record, the limited number of observations during daylight in wintertime does not allow the calculation of monthly means for latitudes higher than about 55°N during the full year. Subsequently, the data are set to be missing

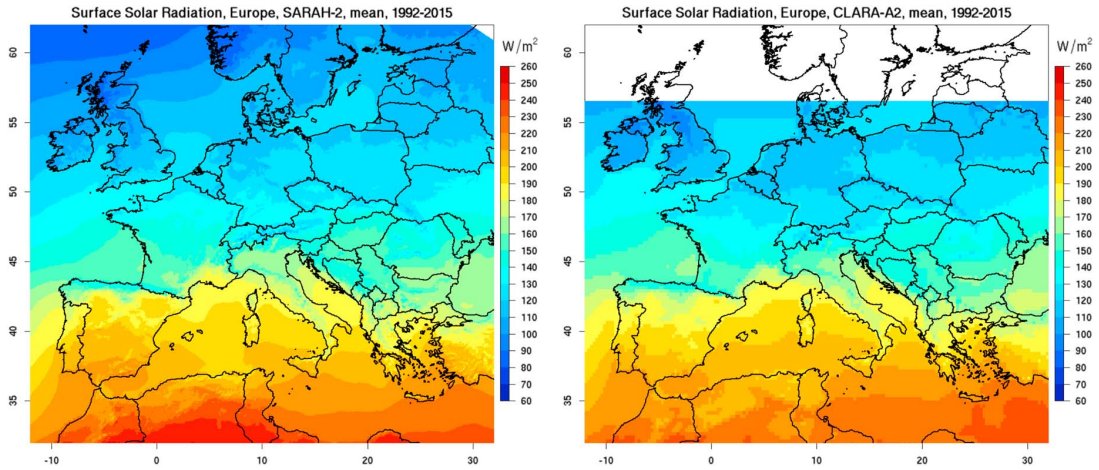

Figure 2. Mean surface solar radiation (W/m^2) (1992–2015) based on the (left) SARAH-2 and (right) CLARA-A2 climate data record.

in the CLARA-A2 climate data record of SSR for the corresponding area during twilight situations, as can be observed in Figure 2.

The validation of the CLARA-A2 monthly solar radiation data with the station data reveals on average a negative bias of −0.4 W/m^2 and a MAD of 7.3 W/m^2 (cf. Table 2). The SARAH-2 monthly SSR data have a positive bias of +2.7 W/m^2 and a MAD of 6.9 W/m^2. The correlation coefficient of monthly anomalies is 0.88 for CLARA-A2 and 0.89 for SARAH-2, documenting that both data records are well suited for the monitoring of monthly anomalies.

The scatterplots of the monthly anomalies derived from CLARA-A2 and SARAH-2 versus the station data are shown in Figure 3, where it is distinguished between the time periods before and after 1992. In 1992, the temporal sampling of the CLARA-A2 climate data record is improved by the availability of a second AVHRR sensor (Karlsson et al., 2017b). As shown in Figure 3 (bottom), the correlation of anomalies substantially increased after 1991 from 0.848 to 0.904. For this reason, in the following analysis the first 10 years of the CLARA-A2 climate data record (1982–1991) is left out to ensure a high temporal stability of the satellite data. Moreover, there are, depending on latitude, up to 50% missing data before 1991 in the CLARA-A2 SSR and as a consequence the absolute bias for the early years increases to about 10 W/m^2 for CLARA-A2, which is more than 30% higher than for the period after 1991 (see Table 2). The correlation of anomalies is around 0.90 for both periods for the SARAH-2 climate data record (cf. Figure 3) allowing the analysis of SARAH-2 for the full period of 1983–2015 in this study.

Overall, the basic evaluation of the CM SAF CLARA-A2 and SARAH-2 climate data records highlights their high quality and accuracy, which allows a detailed analysis of SSR using these satellite-based climate data records provided by the CM SAF.

Table 2
Results of the Validation of Monthly SARAH-2 and CLARA-A2 SSR Data With Reference to Station Data in Europe

	1983–1991		1992–2015		1983–2015	
	MAD	cor	MAD	cor	MAD	cor
CLARA-A2	9.7	0.85	6.5	0.91	7.3	0.88
SARAH-2	8.3	0.89	6.4	0.90	6.9	0.89

Note. MAD = mean absolute deviation (W/m^2) and cor = Pearson's correlation coefficient of the anomaly series.

5. Trend and Variability Analysis

In this part, variability and trends of SSR derived from the CM SAF's SARAH-2 and CLARA-A2 climate data records are evaluated using the station data. Further, the spatial distribution of trends based on the satellite data records is shown.

The mean anomaly time series of SARAH-2, CLARA-A2, and the stations for the 53 European locations are shown in Figure 4. It is thereby distinguished between the time periods of 1983–2015 and 1992–2015 (as noted in section 4). Figure 4 shows that the time series of monthly anomalies agree well between the data records even though the differences are larger in some periods, for example, around 1990 between

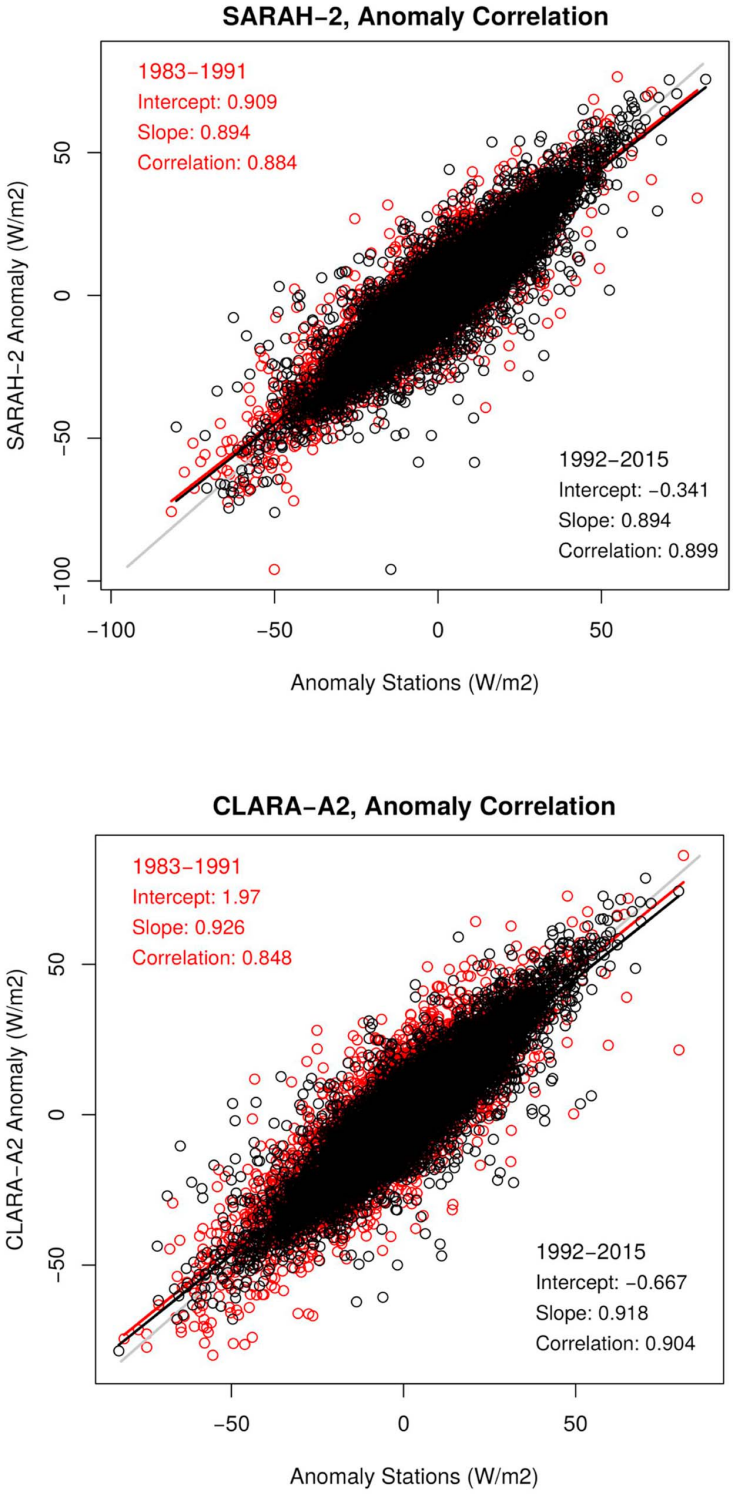

Figure 3. Scatterplot of monthly anomalies of surface solar radiation (W/m^2) of (top) SARAH-2 and (bottom) CLARA-A2 versus station data, including correlation coefficient, slope, and intercept of the regression line. The red color refers to the 1983–1991 period, while the black color refers to the 1992–2015 period.

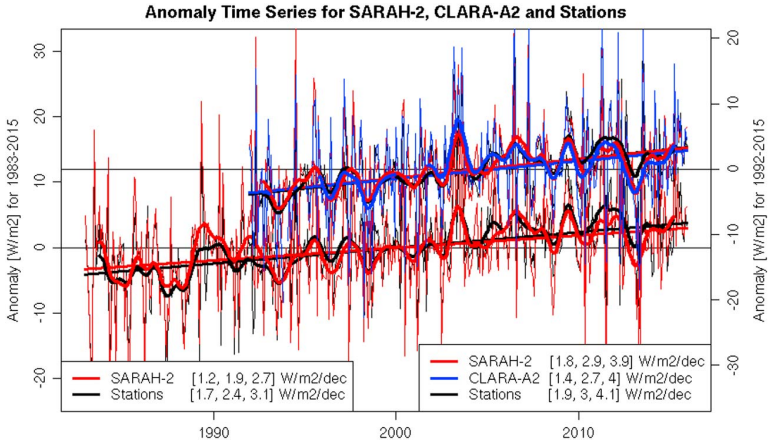

Figure 4. Mean monthly anomaly (W/m^2) time series for the time periods of 1983–2015 (lower lines, *y* axes on the left) and 1992–2015 (upper lines, *y* axis on the right). Additionally shown are the linear trends (solid straight lines) and the smoothed time series (using 12 month Gauss filter) for (black) stations, (red) SARAH-2, and (blue) CLARA-A2 (only for the time period 1992–2015). The values in the brackets show lower 95th percentile, mean trend, and upper 95th percentile. Note that the *y* axes are shifted by 12 W/m^2 from each other.

SARAH-2 and the station-based data. Possible reasons for these slightly larger differences are satellite changes, the disregard of the aerosol radiative effect of the Pinatubo eruption in 1991, or other unknown issues in either the satellite or the station data.

Regarding the linear trends, all three data records agree reasonably well for both the longer and shorter time period (cf. Table 3 and Figure 4), even though both SARAH-2 and CLARA-A2 use an aerosol climatology as input. All data records exhibit positive trends in SSR between 1.9 and 2.4 W/m^2/decade for the period 1983–2015 and between 2.7 and 3.0 W/m^2/decade for the time period 1992–2015. The trends in the station data are overall larger than in the satellite data, while the SARAH-2 trends are somewhat closer to those observed at the stations than the trends derived from CLARA-A2. As shown in Figure 4, the mean trends do agree within their confidence intervals, as the intervals are overlapping each other.

A way to analyze trends during different time periods is by using running-trend analysis as depicted by so-called Trendraster-plots. A Trendraster-plot for the 53 station mean SSR and of the corresponding data of SARAH-2 and CLARA-A2 (at the station locations) is shown in Figure 5. All three Trendraster-plots of SARAH-2, CLARA-A2, and the stations agree in an overall brightening in Europe, shown by the red squares in the lower right part of the Trendraster-plots, which represent the trends of the longest time periods.

Further, there is not only a reasonable agreement in the overall positive trends, but there is also agreement in the shorter-term trends, that is, the decadal variability. In the early years, from 1983 to the late 1990s there is a positive trend in SSR, which is followed by a zero or slightly negative trend during the time period of the late 1980s until about 2002. From the mid-1990s to the mid-2000s the trends are positive again with values between 6 and 8 W/m^2/decade consistent between the data records. During the latest years (i.e., after circa 2006) the SSR trends are small. The most positive trends are found in the 1990s in the CLARA-A2 climate data

Table 3
Absolute (W/m^2/decade) and Relative (%/decade) Trends of SARAH-2, CLARA-A2, and the Station Data During the Time Periods of 1983–2015 and 1992–2015 for the Five Regions Analyzed

Time period	Data	CE	CW	NW	S	N
1983–2015	Stations	3.0 (2.4%)	2.9 (1.9%)	1.7 (1.6%)	5.0 (2.7%)	2.6 (2.4%)
	SARAH-2	2.4 (1.9%)	2.0 (1.3%)	1.8 (1.8%)	2.0 (1.0%)	2.5 (2.4%)
1992–2015	Stations	2.6 (2.0%)	3.3 (2.2%)	2.8 (2.7%)	5.7 (3.0%)	2.0 (1.8%)
	SARAH-2	2.7 (2.0%)	2.8 (1.8%)	2.9 (2.9%)	1.8 (0.9%)	1.9 (1.7%)
	CLARA-A2	2.4 (1.8%)	3.1 (2.0%)	3.7 (3.4%)	1.9 (1.0%)	/

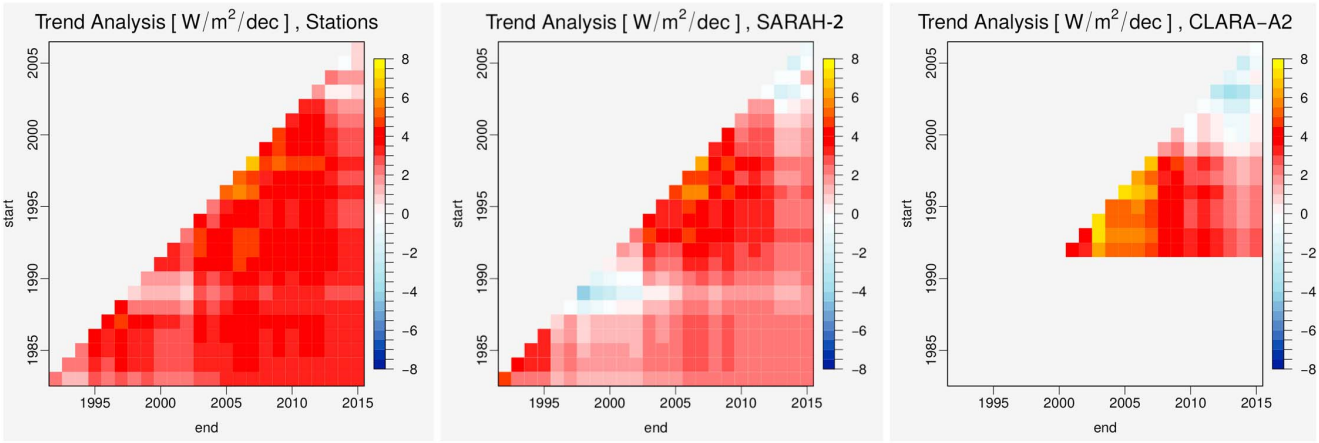

Figure 5. Trendraster-plots of mean SSR trends derived from (left) stations, (middle) SARAH-2, and (right) CLARA-A2. The *y* axis denotes the start years, and the *x* axis shows the end years of the individual trends. Trendrasters show linear trends (W/m^2/decade) during time periods of at least 10 years (at the diagonal); the trend over the maximum time period analyzed (33 years for station data and SARAH-2 and 24 years for CLARA-A2) is shown by the pixel at the lower right end.

record with values of up to 8 W/m^2/decade. The mainly zero (or slightly negative) trends of SSR during about 1989–2000 are smaller in the SARAH-2 climate data record than those derived from the station data.

The regional trends over the 33 year time period are shown in Figure 6. For each of the five regions (cf. Figure 1), a box plot is used to depict the distribution of the linear trends for the locations in the different regions. Each box plot shows the mean and the median of the trends as well as quartiles, percentiles, and outliers. Figure 6 compares the regional trends during the time period 1983–2015, when SARAH-2 and the stations are used, and during the shorter time period 1992–2015, when also CLARA-A2 is used. It is shown that the mean regional trends are all positive and are mostly ranging between 2 and 4 W/m^2/decade. In all regions, except the region south, the trends between the two satellite climate data records and the stations agree well (see also Table 3). An exception is found in the region south, where the trends based on station data are much larger than in the CM SAF's satellite climate data records, for both analyzed time periods. In the region south, the mean trends based on the station data are in the order of 5 to 6 W/m^2/decade, while the trends based on SARAH-2 and CLARA-A2 data are consistently lower in the order of 2 W/m^2/decade. The larger spread in the trends among the stations in region south is evident, in particular, for the shorter time period (cf. outliers in Figure 6), when trends range from 3 to 10 W/m^2/decade.

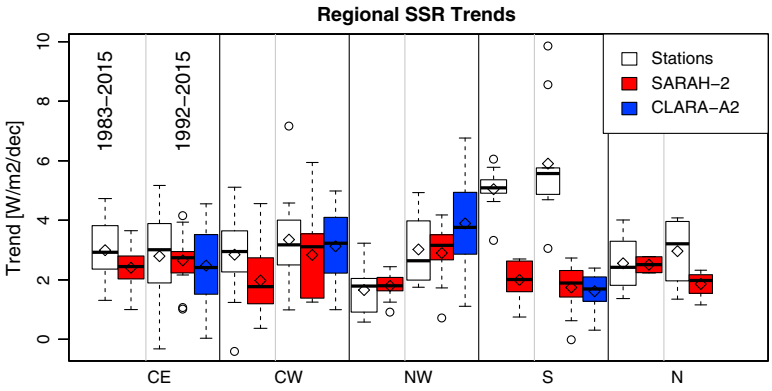

Figure 6. Box plot of the regional trends (W/m^2/decade) of surface solar radiation at the station locations (white) based on stations, (red) SARAH-2, and (blue) CLARA-A2 data, including mean trends (diamonds). Outliers are shown as dots. Regions: CE = central east, CW = central west, NW = northwest, S = south, and N = north. For each region the plot area is divided into trends for the full time period 1983–2015 (for stations and SARAH-2) and trends for the time period 1992–2015 (for stations, SARAH-2, and CLARA-A2).

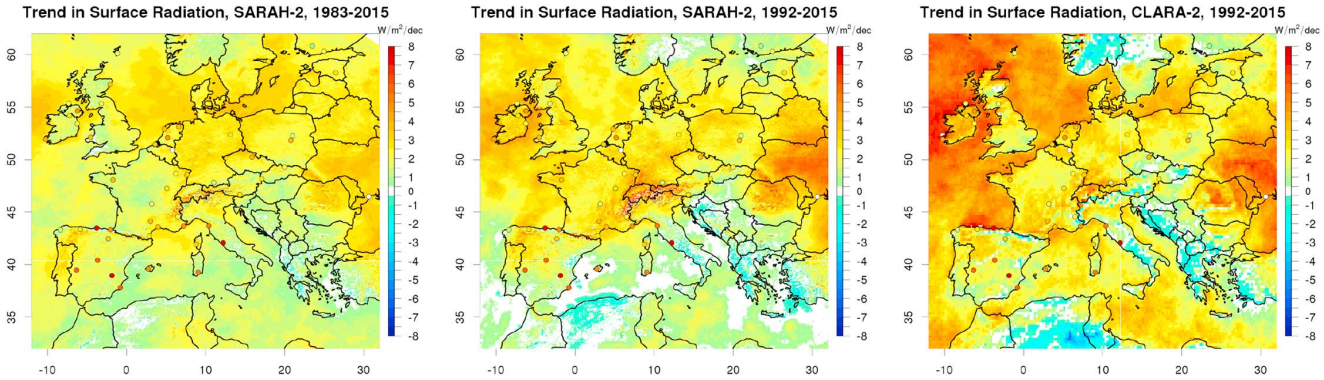

Figure 7. Spatial distribution of the linear trends (W/m^2/decade) of surface solar radiation during 1983–2015 for (left) SARAH-2 and during 1992–2015 for (middle) SARAH-2, and (right) CLARA-2. The respective trends for the 53 stations are shown as colored dots.

A worthwhile characteristic of satellite data is its provision of spatially complete information. The spatial pattern of the linear trends of SSR in Europe given by the CM SAF SARAH-2 and CLARA-A2 is shown in Figure 7. For comparison the SSR trends of the station data are added. Figure 7 (left) the trend of SARAH-2 for the full 33 year period is shown. The largest positive trend is found in eastern Europe (especially east of the Carpathian Mountains). Strong positive trends of SSR are also visible in parts of central Europe and over the North and Baltic Seas. Some regions experience a low or negative trend during the time period 1983–2015, for example, parts of France and Great Britain.

Figure 7 also provides the SSR trends for the time period 1992–2015 for the CLARA-A2 and the SARAH-2 data records. There is a remarkable agreement between both data records in the mean trends at the stations (cf. Figure 4) and in its spatial pattern, especially over land. During the time period 1992–2015 the most positive trends can be found in eastern Europe while slightly negative trends are derived in parts of the eastern Mediterranean region in both data records. Over the oceans, especially over the Atlantic Ocean and the North Sea, the trends are more positive in the CLARA-A2 climate data record than in the SARAH-2 climate data record. The CLARA-A2 SSR also has a more distinct land-ocean difference in trends compared to the SARAH-2 SSR.

The mean seasonal trends of SSR for the five regions are shown in Figure 8. In all regions, except in the region south, the strongest positive trends in SSR are observed in the spring season, with values in the range of about 4 to 6 W/m^2/decade. In summer, the trends are also positive, with extreme positive trends given by the station data in the region south, where the mean trend is around 9 W/m^2/decade, in line with results from Sanchez-Lorenzo et al. (2015) and Manara et al. (2016). Again, we find an overall tendency of a slight underestimation of the positive trends of the satellite data with reference to the station data, mainly in spring and summer. Based on the sign and magnitude of the SSR trends (cf. Figure 8), we conclude that there is a reasonable agreement between the CM SAF's satellite and the station data. Notable exception is the region south during summer, which will be discussed in more detail in section 5.2.

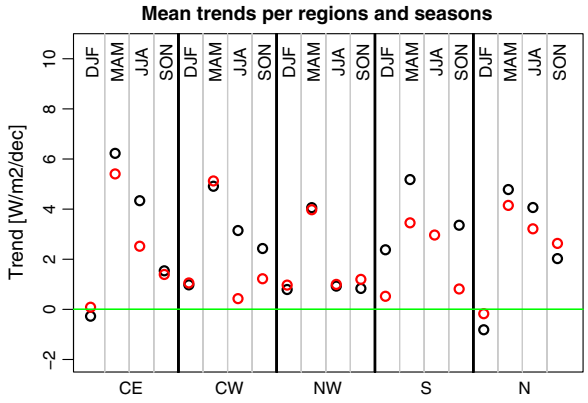

Figure 8. Trends (W/m^2/decade) of surface solar radiation of (black) stations and (red) SARAH-2 data, shown separately for region and season during the full time period of 1983–2015. Regions: CE = central east, CW = central west, NW = northwest, S = south, and N = north.

Similar to the trend over the 33 years time period shown in Figure 8, Figure 9 presents the regional and seasonal trends for the shorter time period of 1992–2015, for which the CLARA-A2 climate data record is analyzed as well. We find larger differences in the trends of the different data records for the shorter time period. As expected, the absolute trends in the different regions and seasons are partly different to the ones derived for the 33 year time period (Figure 8). For example, in the region central west, the strongest positive trends between 1992 and 2015 occur in autumn and not in spring. Again, disagreements in the trends are obvious in the region south. Especially during the summer season, the station data show strong positive trends of more than 10 W/m^2/decade (see dot at the top of Figure 9), while the satellite-based data indicate trends of about 3

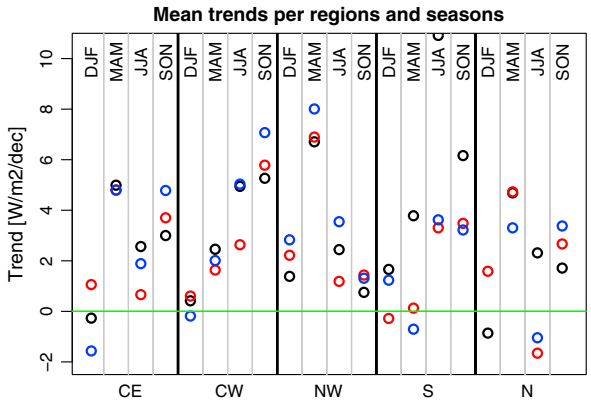

Figure 9. Trends (W/m^2/decade) of surface solar radiation of (black) stations, (red) SARAH-2, and (blue) CLARA-A2 data, shown separately for region and season during the time period of 1992–2015. Regions: CE = central east, CW = central west, NW = northwest, S = south, and N = north.

to 4 W/m^2/decade. Figure 9 also shows that there are some negative trends for the time period 1992–2015, for example, in the region north's winter season. Still, the trends in the majority of regions and seasons are positive, documenting the general increase of SSR. There is a good agreement between the three data records in the regions central east, central west, and northwest, while differences are larger in the regions south and north.

The spatial distribution of the seasonal trends in SSR based on the CMSAF's climate data records are shown in Figures 10 and 11. In Figure 10, the trends based on SARAH-2 and the station data are shown for the time period 1983–2015. It is obvious that there are large differences between the trends in the different seasons. The smallest trends (negative in some regions like eastern Europe) are observed in winter, while the largest ones are observed in spring (cf. Figure 10, top right) when in large areas of central and eastern Europe the trends exceed 5 W/m^2/decade. In summer, the trends remain positive in the east, but some areas in the west, namely, parts of France and Great Britain, show slightly negative trends, in line with the station data (cf. Figure 10, bottom left). In autumn, there are small positive trends in most of Europe, while the trends are mainly negative in the southeast of Europe. These negative trends in autumn (i.e., in the Balkan states) have also been found by Alexandri et al. (2017) for the time period 1983–2013.

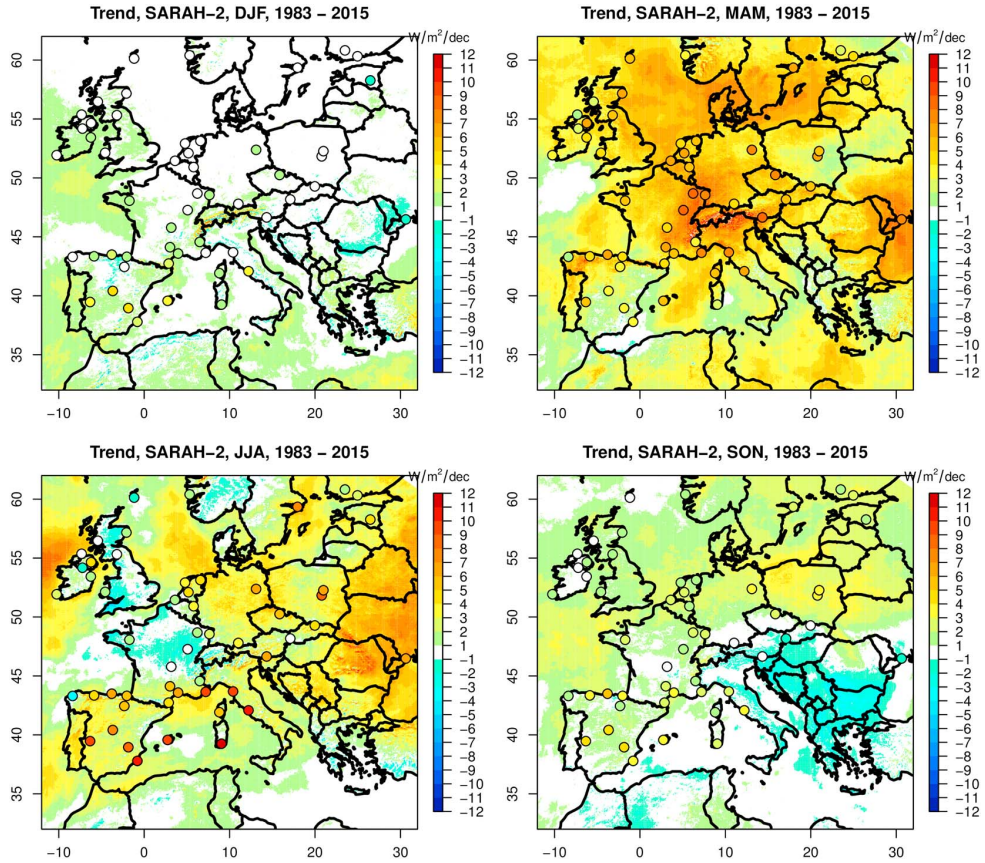

Figure 10. Spatial distribution of the linear trends (W/m^2/decade) of surface solar radiation during 1983–2015 for the four seasons (DJF, MAM, JJA, and SON) based on the SARAH-2 climate data record. The trends for the respective season and time period given by the 53 stations are shown as colored dots.

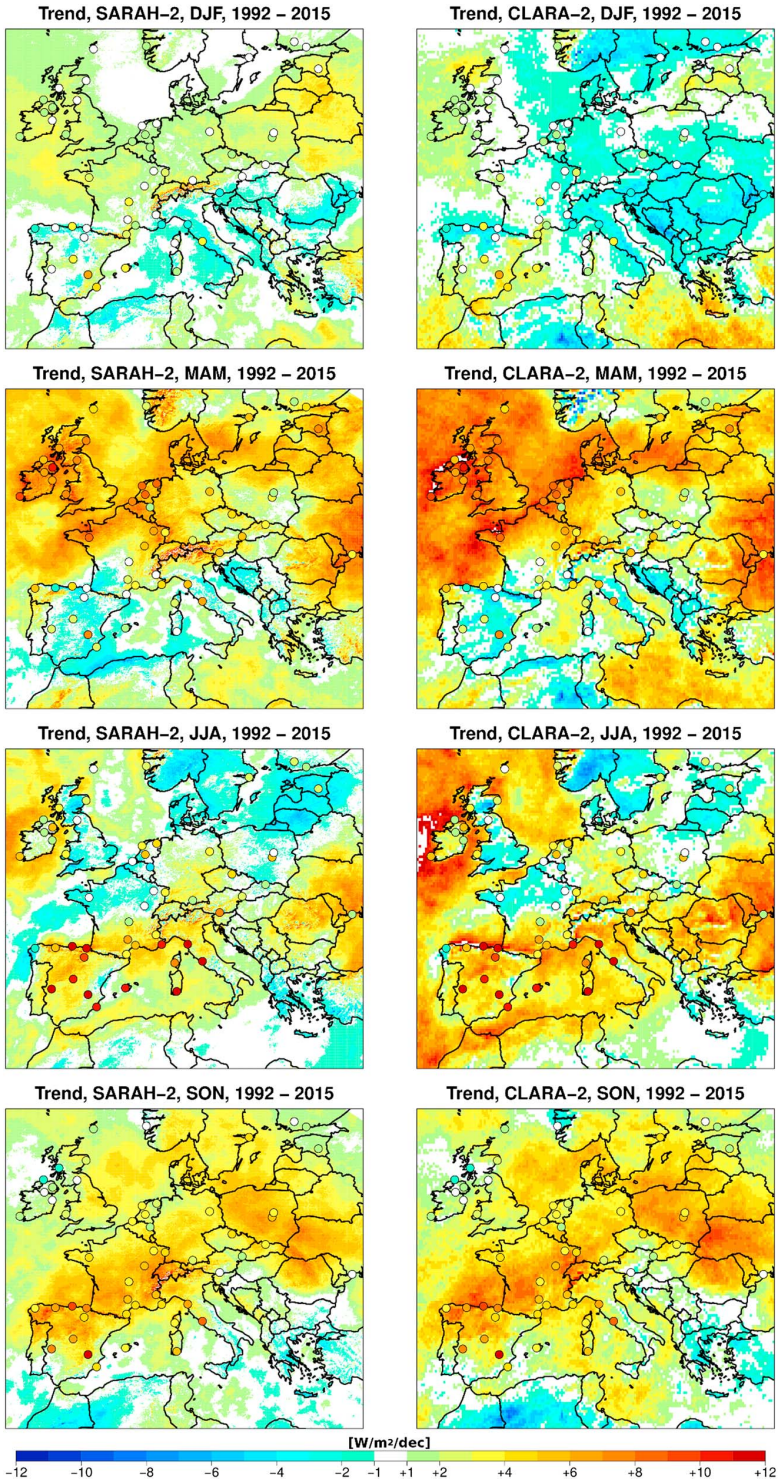

Figure 11. Spatial distribution of the linear trends (W/m^2/decade) of surface solar radiation during 1992–2015 for the four seasons (DJF, MAM, JJA, and SON) (top to bottom) based on the (left column) SARAH-2 and (right column) CLARA-A2 climate data records. The trends for the respective season and time period given by the stations are shown as colored dots.

To compare the trends derived from SARAH-2 and CLARA-A2, the spatial trend maps are shown in Figure 11 for the common time period of 1992–2015. Figure 11 reveals similar spatial patterns of seasonal trends in Europe of SARAH-2 and CLARA-A2, which indicates a consistency of the independently derived climate data records. It should be noted that the overall agreement in the trends between the satellite and stations data is also valid for the individual stations (with the exception of region south). By comparing the seasonal trend patterns given in Figures 10 and 11, it is visible that the spatial variability of trends in Europe is large, especially on shorter time scales. In general, it has been found that the trends can substantially vary, even if the time period considered is only slightly changed.

Motivated by the results shown in Figures 8 and 9, we present additional analysis for the regions north and south in the following sections.

5.1. Focus: Region North

In the region north the trends derived from the satellite-based data records and from the station data agree in spring and autumn in the region north, but there are larger differences in the summer and winter season, in particular, during the time period 1992–2015 (as shown in Figure 9). In this period, during the summer season, both SARAH-2 and CLARA-A2 have negative trends of −1 to −2 W/m^2/decade, while the station data have a positive trend of 2 to 3 W/m^2/decade. In the winter season the differences are the opposite with positive values for SARAH-2 and negative trends based on the station data (no CLARA-A2 data analyzed here due to missing data). However, for the full time period of 1983–2015, the trends of SSR agree (cf. Figure 8).

To further investigate, these differences between the trends the Trendraster-plots for region north are shown for the winter and summer season for both the station data and SARAH-2 (cf. Figure 12). In winter, it is visible that even though the long-term trend agrees (no trend during the period 1983–2015), there are substantial differences on the shorter term (cf. Figure 12, upper part). Most obvious are the relatively strong positive trends during the winter season in the SARAH-2 data starting in mid-1990s onward. During that period, SARAH-2 shows a larger positive trend in SSR than the surface observations. Relative trends can reach up to +15% SSR per decade, which is due to the low absolute values SSR levels in winter. One possible reason for the trend overestimation by SARAH-2 is related to the fact that snow on the ground can be misinterpreted as clouds in the satellite retrieval scheme used in the generation of SARAH-2 resulting in an underestimation of SSR under snow-covered conditions. A change in the snow cover would result in an artificial change in SSR in the SARAH-2 climate data record, because the underestimation of SSR under snow-covered conditions would be reduced. Hence, the negative trend in snow cover during the mid-1990s in the region north (Brown & Robinson, 2011) might have contributed to the positive trend in the SARAH-2 data record in wintertime SSR in the region north. Nevertheless, it should be noted that a slight positive trend is also observed by the stations during that time period even if it is smaller compared to SARAH-2. However, at this stage we cannot rule out an impact of the change in the satellite instruments used in the generation of SARAH-2 in 2006 on the differences in the trends we are finding in the region North in winter.

During the summer, the trends are higher than during the winter, and the trend is overall positive in both the station data and the SARAH-2 data (cf. Figure 12, lower part). The temporal variability of the trends is high in both data records. The SARAH-2-based trends ending after 2007 tend to be smaller than the trends based on station data. Possible reasons are a change in the onset of snow coverage or an inhomogeneity from the change in the satellite instruments.

Overall, we conclude that the trends based on satellite data in the region north need to be considered with care. The study of Riihelä et al. (2015) finds a good correspondence between satellite- and station-based trends but did not assess seasonal trends, where the larger differences appear in the present study.

5.2. Focus: Region South

The region south exhibits the largest differences in trends between the satellite climate data records and the station data (cf. Figures 6, 8, and 9). To get more insights, additional Trendraster-plots based on SARAH-2, CLARA-A2, and the station data for the region south are presented in Figure 13 for all seasons. In winter, spring, and autumn, there is a general agreement between the satellite data and the station data, even though there is a small tendency of the satellite data to underestimate the trends in SSR with reference to the station data. For the common time period of 1992–2015, the SARAH-2 Trendrasters compared better with the station-based Trendraster than the CLARA-A2 Trendrasters.

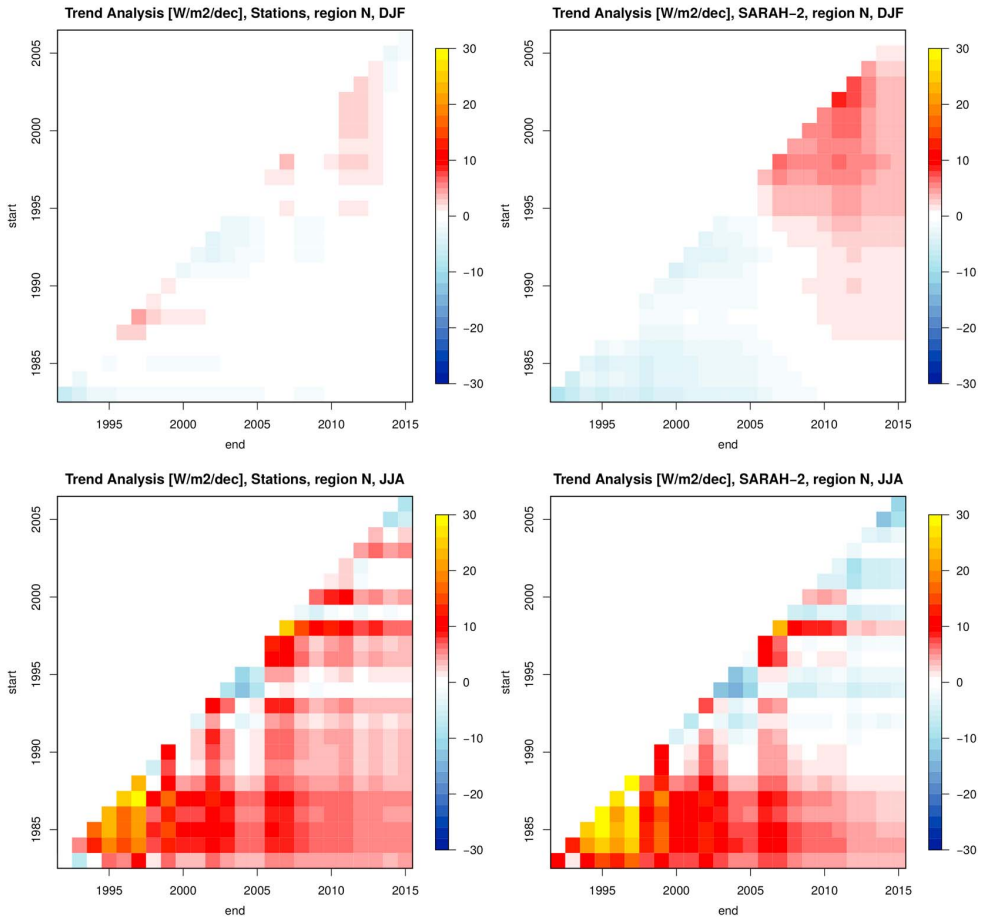

Figure 12. Trendraster-plots of mean SSR trends derived from (left) stations and (right) SARAH-2, for the (top) winter and (bottom) summer season for the region north. The *y* axis denotes the start years, and the *x* axis shows the end years of the individual trends. Trendrasters show linear trends (W/m^2/decade) during time periods of at least 10 years (at the diagonal); the trend over the maximum time period analyzed is shown by the pixel at the lower right end.

The largest differences are evident in the summer season (see Figure 13, third row), where SARAH-2 and CLARA-2 clearly disagree with the station data. In fact, the satellite data show a much smaller positive trend than the station data. It is remarkable that SARAH-2 and CLARA-A2 agree well for the summer season with each other, even though they are based on different sensors on different satellites and so they are independent.

However, there is one relevant aspect that both SARAH-2 and CLARA-A2 have in common: the use of a constant monthly climatology of aerosol information as input (Müller, Pfeifroth, & Traeger-Chatterjee, 2015). A decreasing aerosol load, as, for example, reported in Spain (Sanchez-Romero et al., 2016) or over the mainland Europe (Ruckstuhl et al., 2008) since the 1980s would lead to a positive trend in SSR, due to the reduced direct aerosol effect on SSR, which would not be captured by SARAH-2 or CLARA-A2. This fact might be one explanation of the underestimation of the trend by both SARAH-2 and CLARA-A2 with reference to the station data. This hypothesis seems to be confirmed also considering recent results published by Georgoulias, Alexandri, Kourtidis, Lelieveld, Zanis, and Amiridis (2016). They investigated the spatiotemporal evolution (since 2000s) of the aerosol optical depth over the greater Mediterranean region finding that the subregions with the stronger negative aerosol optical density (AOD550) trend are the central Mediterranean and the Iberian Peninsula, attributed to the positive precipitation trends all over the region and to the decrease of anthropogenic emissions in the area.

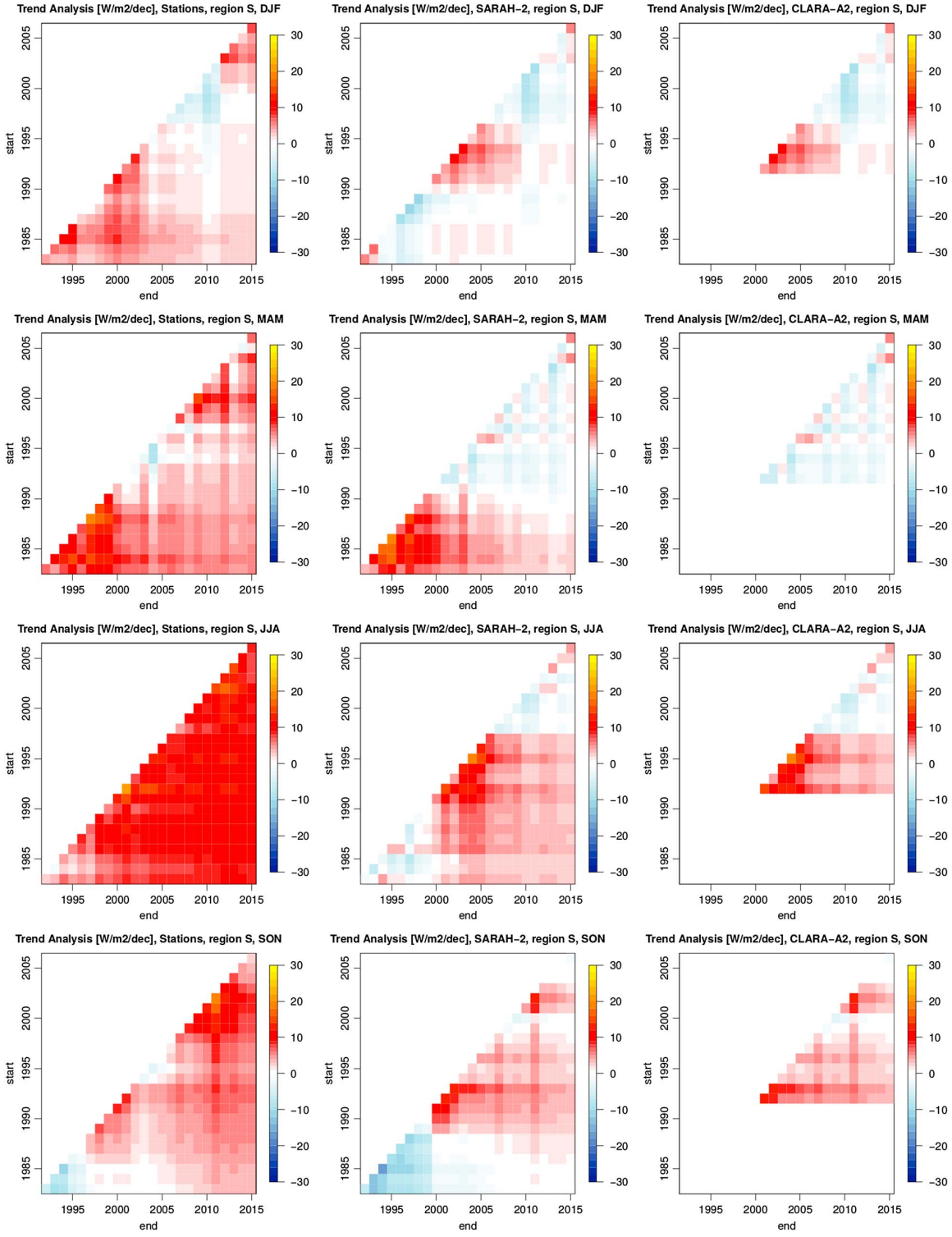

Figure 13. Trendraster-plots of mean SSR trends derived from (left) stations, (middle) SARAH-2, and (right) CLARA-A2 for the seasons (from top to bottom: DJF, MAM, JJA, and SON) for the region south. Trendrasters show linear trends (W/m^2/decade) during time periods of at least 10 years (at the diagonal); the trend over the maximum time period analyzed (33 years for station data and SARAH-2 and 24 years for CLARA-A2) is shown by the pixel at the lower right end.

On the other hand, the major part of the variability and trends in Europe is reasonably captured by the CM SAF's SARAH-2 and CLARA-A2 climate data records, including the region central east. The region south's summer season is an exception in this respect. However, it should be considered that in this region, the SSR is likely being more affected by potential changes of the aerosol direct effect (Nabat et al., 2014), as clear-sky days are more frequent in the Mediterranean summer than in other European areas. This is coherent with the findings of Kambezidis et al. (2016), who found higher values under clear skies (without aerosols but including clouds) compared to those under clear skies (without clouds but including aerosols) using reanalysis data of surface net shortwave radiation during June–August, indicating that aerosols attenuate more the shortwave radiation compared to clouds over the Mediterranean in summer. Moreover, a positive trend in clear-sky SSR in Europe has been found by Bartók (2017) during the time period 2001–2012, which is partly attributed to a reduced aerosol load. This signal is confirmed both by Manara et al. (2016) for the Italian territory and by Sanchez-Lorenzo and Wild (2012) over Switzerland. The former found during the brightening period stronger positive SSR tendencies under clear-sky conditions than under all-sky conditions suggesting that cloud cover variations have partially masked the variations caused by aerosol variations (both anthropogenic and natural) especially during winter and autumn. The latter found in the clear-sky SSR series during the subperiod 1981–2010 a positive trend especially in spring and summer attributing them to the direct aerosol effect (Ruckstuhl et al., 2008; Ruckstuhl & Norris, 2009).

While the neglect of the change in the aerosol loading in the satellite retrieval provides a possible and likely reason for the underestimation of the trend by the satellite data sets, the impact of the change in the instrumentation to measure the SSR at the surface stations has not yet been quantified and a possible impact on the trend calculation based on station data cannot be ruled out at this stage.

6. Discussion and Conclusions

In this study, the variability and trends of surface solar radiation are analyzed in Europe during the time period 1983–2015. Here the CM SAF's SARAH-2 and CLARA-A2 climate data records of SSR are compared to surface observations to assess their ability to reproduce the surface observations. It is found that the overall variability and the trends agree well between the CMSAF's SARAH-2, CLARA-A2, and the station data in Europe. It is important to mention that the CLARA-A2 and the SARAH-2 data records are independent from each other, as they are based on different satellite systems and algorithms. So the agreement in trends and variability (especially over the continent) for the time period for which both data records are used (1992–2015) is remarkable and documents the high quality of SARAH-2 and CLARA-A2 (see, e.g., Figures 7 and 11). Possible reasons for the remaining differences between the SSR trends in the satellite and station data might be connected to the neglection of changes in the aerosol loading (e.g., Bartók, 2017; Sanchez-Lorenzo et al., 2017) and to effects of a change in snow cover, as described in section 5.1. It is important to mention that the clear-sky radiation given by SARAH-2 (and CLARA-A2), which are only driven by the time varying water vapor input, does show negligible trends of SSR of mostly below ± 0.2 W/m^2/decade (not shown), consistent with previous results (Posselt et al., 2014). The largest negative trends in the SARAH-2 clear-sky radiation are found the Balkan region and in southeastern Europe with up to -0.6 W/m^2/decade, which is still much smaller than most of the all-sky SSR trends.

The CM SAF's SARAH-2 and CLARA-A2 have reached a high quality and stability that enables the analysis of variability and trends in SSR. The observed positive trends of SSR (considering both the satellite data records and the station data) are about 1.9 to 2.4 W/m^2/decade. Stronger positive trends of about 2.7 to 3.0 W/m^2/decade are observed during the shorter time period of 1992–2015 (cf. Figure 4). Figure 5 shows that also the variability of SSR agrees between the CM SAF's satellite climate data records and the station data. The spatial view on the long-term SSR trends reveals that the strongest brightening is found for the spring season and mainly in eastern Europe and in the northwestern Europe (cf. Figures 7 and 10). Overall, the spatial trend patterns and its seasonal variability are similar to findings by Sanchez-Lorenzo et al. (2017) over the 1983–2010 period. An exception is seen for the summer season in region south, where the trends based on the satellite data records and the station data disagree (cf. Figure 8). There, the positive trend observed by the station data is underestimated by the satellite data (cf. section 5.2). However, the spread between the trends in the station data is also largest in the region south (cf. Figure 6), which indicates that regional to local causes for trends might potentially exist as well. In general, even though care has been taken in the data compilation, remaining data inhomogeneities (e.g., due to instrumental changes) in either satellite or stations data cannot be fully excluded.

Aerosol information is kept constant for both SARAH-2 and CLARA-A2 because of the nonavailability of high-quality aerosol information for the full time period of the satellite data at the time of data generation (Müller, Pfeifroth, & Traeger-Chatterjee, 2015). It is important to note, that, even though the aerosol information is kept constant within SARAH-2 and CLARA-A2, changes of the aerosol indirect effect are expected to be captured (Müller, Pfeifroth, & Traeger-Chatterjee, 2015), that is, through the changes in cloud brightness and life time.

The Mediterranean region is affected by large aerosol loads for anthropogenic and natural reasons. It is affected by sea-salt aerosols from the Mediterranean Sea and the Atlantic Ocean, pollution aerosols from Europe, dust from the Sahara desert, and biomass burning aerosols from eastern Europe. Moreover, depending on the season, different types of aerosols reach different parts of the region (e.g., dust peaks in spring over the eastern Mediterranean, in summer over the western Mediterranean, and in spring and summer over the transitional region of central Mediterranean) (Floutsi et al., 2016; Georgoulias, Alexandri, Kourtidis, Lelieveld, Zanis, Pschl, et al., 2016; Georgoulias, Alexandri, Kourtidis, Lelieveld, Zanis, & Amiridis, 2016; Kanakidou et al., 2011; Lelieveld et al., 2002). For this reason, the influence of the aerosol direct effect on SSR is supposed to be large in the region south (Bartók, 2017; Kambezidis et al., 2016; Nabat et al., 2014; Sanchez-Lorenzo et al., 2017). This allows to conclude that at least parts of the differences between satellite and station data found in the region south's summer (cf. section 5.2) might be attributed to the missing of changes in the aerosol direct effect in the satellite data records (Sanchez-Lorenzo et al., 2017). Sanchez-Lorenzo et al. (2017) also found, for a shorter time period, that for the majority of Europe the differences in trends between the satellite-based SSR data and station data were small, even though a constant aerosol approach (Posselt et al., 2012) has been used in generating the satellite data record, which is overall in line with the findings of this study. For the time period since the 2000s Mateos et al. (2014) state that over the Iberian Peninsula three fourths of the SSR trend is explained by changes in clouds.

Another peculiarity is found in the region north, where the running-trend analysis revealed that for the time period from the mid-1990s onward, the trends are overestimated by the SARAH-2 climate data record with reference to the station data. As noted in section 5.1, a reduction in snow cover could potentially lead to a positive trend in SSR in the satellite data records.

However, for the other regions in Europe, the trends and variability of SSR between satellite and station data agree reasonably well for all seasons, which suggests that aerosol changes (especially aerosol direct effects) play only a minor role for the observed trends in SSR in these regions. Further, based on the algorithms and their input used to generate the SARAH-2 and CLARA-A2 climate data records (cf. Karlsson et al., 2017b; Müller, Pfeifroth, Traeger-Chatterjee, Trentmann, et al., 2015) and based on an analysis of trends in water vapor, which is found to be negligible, it can be concluded, that the large majority of the observed positive trends in SSR in Europe are due to changes in clouds. This finding is also consistent with the results of Sanchez-Lorenzo et al. (2017), based on satellite- and surface-based cloud data records, including the first version of the CLARA data record, who found a decrease in cloud coverage in Europe. The results are robust when using the CLARA-A2 data record (not shown).

In general, the changes in cloud radiative effects reproduced by SARAH-2 and CLARA-A2 can be due to natural cloud variability and/or changes in the aerosol effects on clouds, and consequently, aerosol effects cannot be ruled out completely through indirect aerosol effects. Nevertheless, it is worth noting that at present most of the literature using ground-based data or climate model simulations have reported that the major cause of the brightening in Europe, especially in central Europe, is related to the direct aerosol effects via a decrease in anthropogenic aerosol emissions since the 1980s (e.g., Nabat et al., 2014; Norris & Wild, 2014; Philipona et al., 2009; Zubler et al., 2011). Boers et al. (2017) found that positive trends in SSR in the Netherlands are due to changes in both aerosols and clouds.

Consequently, the results of this study add new information to the available literature. Also, in some previous studies the dimming period observed between the 1950s and 1980s was mainly attributed to cloud changes instead of direct aerosol effects (Liepert, 1997). Stjern et al. (2009) and Parding et al. (2016) also found that changes in clouds are the main reason for trends in SSR in northern Europe, and in the Mediterranean observations indicate fewer clouds for the period 1971 to 2005 (Sanchez-Lorenzo et al., 2017). In the United States, observed positive trends in SSR since the 1990s are also mainly attributed to changes in cloud cover (Augustine & Dutton, 2013).

While it can be assumed that the quality of the satellite-based data records as documented here is representative also for other regions available in the satellite data record, a comparison with high-quality surface data is always recommended when possible. Since no reliable data are available for large parts of the world, satellite data will remain the only observational source of climatic information.

In any case, further research is needed to consolidate the reasons and the mechanisms behind the variability and trends in SSR since the 1980s in Europe. This study documents the quality of the satellite-derived data records to help addressing those topics in future studies and investigations. In particular, the capturing of the spatial structure of the trends in SSR might help to identify the relevant processes.

Acknowledgments
The used EUMETSAT CMSAF's SARAH-2 and CLARA-A2 climate data records are freely available via http://www.cmsaf.eu/wui. The majority of station data used (except for some Spanish and Italian stations) can be obtained from the GEBA archive via http://www.geba.ethz.ch/. The authors thank the data providers for free data access. A. S. L. was supported by post-doctorial fellowships (JCI-2012-12508 and RYC-2016-20784) and a project (CGL2014-55976-R) funded by the Spanish Ministry of Economy, Industry and Competitiveness.

References

Alexandri, G., Georgoulias, A. K., Meleti, C., Balis, D., Kourtidis, K. A., Sanchez-Lorenzo, A., … Panis, P. (2017). A high resolution satellite view of surface solar radiation over the climatically sensitive region of eastern Mediterranean. *Atmospheric Research*, *188*, 107–121. https://doi.org/10.1016/j.atmosres.2016.12.015

Augustine, J. A., & Dutton, E. G. (2013). Variability of the surface radiation budget over the United States from 1996 through 2011 from high-quality measurements. *Journal of Geophysical Research: Atmospheres*, *188*, 43–53. https://doi.org/10.1029/2012JD018551

Bartók, B. (2017). Aerosol radiative effects under clear skies over Europe and their changes in the period of 2001–2012. *International Journal of Climatology*, *37*(4), 1901–1909. https://doi.org/10.1002/joc.4821

Boers, R., Brandsma, T., & Siebesma, A. P. (2017). Impact of aerosol and clouds on decadal trends in all-sky solar radiation over the Netherlands (1966–2015). *Atmospheric Chemistry and Physics*, *17*, 8081–8100. https://doi.org/10.5194/acp-17-8081-2017

Brown, R. D., & Robinson, D. A. (2011). Northern Hemisphere spring snow cover variability and change over 1922–2010 including an assessment of uncertainty. *The Cryoshpere*, *5*, 219–229. https://doi.org/10.5194/tc-5-219-2011

Brunetti, M., Maugeri, M., Nanni, T., Auer, I., Böhm, R., & Schöner, W. (2006). Precipitation variability and changes in the greater Alpine region over the 1800–2003 period. *Journal of Geophysical Research*, *111*, D11107. https://doi.org/10.1029/2005JD00667

Floutsi, A. A., Korras-Carraca, M. B., Matsoukas, C., Hatzianastassiou, N., & Biskos, G. (2016). Climatology and trends of aerosol optical depth over the Mediterranean basin during the last 12 years (2002–2014) based on Collection 006 MODIS-Aqua data. *Science of The Total Environment*, *551–552*, 292–303. https://doi.org/10.1016/j.scitotenv.2016.01.192

Georgoulias, A. K., Alexandri, G., Kourtidis, K. A., Lelieveld, J., Zanis, P., Pschl, U., … Tsikerdekis, A. (2016). Spatiotemporal variability and contribution of different aerosol types to the aerosol optical depth over the eastern Mediterranean. *Atmospheric Chemistry and Physics*, *16*, 13,853–13,884. https://doi.org/10.5194/acp-16-13853-2016

Georgoulias, A. K., Alexandri, G., Kourtidis, K. A., Lelieveld, J., Zanis, P., & Amiridis, V. (2016). Differences between the MODIS Collection 6 and 5.1 aerosol datasets over the greater Mediterranean region. *Atmospheric Environment*, *147*, 310–319. https://doi.org/10.1016/j.atmosenv.2016.10.014

Gilgen, H., Roesch, A., Wild, M., & Ohmura, A. (2009). Decadal changes in shortwave irradiance at the surface in the period 1960 to 2000 estimated from Global Energy Budget Archive Data. *Journal of Geophysical Research*, *114*, D00D08. https://doi.org/10.1029/2008JD011383

Hartmann, D. L., Ramanathan, V., Berroir, A., & Hunt, G. E. (1986). Earth radiation budget data and climate research. *Reviews of Geophysics*, *24*(2), 1944–9208. https://doi.org/10.1029/RG024i002p00439

Hinkelmann, L. M., Stackhouse Jr., P. W., Wielicki, B. A., Zhang, T., & Wilson, S. R. (2009). Surface insolation trends from satellite and ground measurements: Comparisons and challenges. *Journal of Geophysical Research*, *114*, D00D20. https://doi.org/10.1029/2008JD011004

Huld, T., Moner-Girona, M., & Kriston, A. (2017). Geospatial analysis of photovoltaic mini-grid system performance. *Energies*, *10*, 218. https://doi.org/10.3390/en10020218

Kambezidis, H. D., Kaskaoutis, D. G., Kalliampakos, G. K., Rashki, A., & Wild, M. (2016). The solar dimming/brightening effect over the Mediterranean Basin in the period 1979–2012. *Journal of Atmospheric and Solar-Terrestrial Physics*, *150–151*, 31–46. https://doi.org/doi.org/10.1016/j.jastp.2016.10.006

Kanakidou, M., Mihalopoulos, N., Kindap, T., Im, U., Vrekoussis, M., Gerasopoulos, E., … Moubasher, H. (2011). Megacities as hot spots of air pollution in the East Mediterranean. *Atmospheric Environment*, *45*, 1223–1235. https://doi.org/10.1016/j.atmosenv.2010.11.048

Karlsson, K.-G., Anttila, K., Trentmann, J., Stengel, M., Fokke Meirink, J., Devasthale, A., … Werscheck, M. (2017a). CLARA-A2: CM SAF cLoud, albedo and surface radiation dataset from AVHRR data—Edition 2, Satellite Application Facility on Climate Monitoring. https://doi.org/10.5676/EUM_SAF_CM/CLARA_AVHRR/V002

Karlsson, K.-G., Anttila, K., Trentmann, J., Stengel, M., Fokke Meirink, J., Devasthale, A., … Hollmann, R. (2017b). CLARA-A2: the second edition of the CM SAF cloud and radiation data record from 34 years of global AVHRR data. *Atmospheric Chemistry and Physics*, *17*(9), 5809–5828. https://doi.org/10.5194/acp-17-5809-2017

Kothe, S., Pfeifroth, U., Cremer, R., Trentmann, J., & Hollmann, R. (2017). A satellite-based sunshine duration climate data record for Europe and Africa. *Remote Sensing*, *9*, 429. https://doi.org/10.3390/rs9050429

Lelieveld, J., Berresheim, H., Borrmann, S., Crutzen, P. J., Dentener, F. J., & Fischer, H. (2002). Global air pollution crossroads over the Mediterranean. *Science*, *298*(5594), 794–799. https://doi.org/10.1126/science.1075457

Liepert, B., Fabian, P., & Grassl, H. (1994). Solar radiation in Germany—Observed trends and an assessment of their causes. Pt 1.*Contributions to Atmospheric Physics*, *67*(1), 15–29.

Liepert, B. (1997). Recent changes in solar radiation under cloudy conditions in Germany. *International Journal of Climatology*, *17*(14), 1581–1593.

Manara, V., Brunetti, M., Celozzi, A., Maugeri, M., Sanchez-Lorenzo, A., & Wild, M. (2016). Detection of dimming/brightening in Italy from homogenized all-sky and clear-sky surface solar radiation records and underlying causes (1959–2013). *Atmospheric Chemistry and Physics*, *16*, 11145–11161. https://doi.org/10.5194/acp-16-11145-2016

Mercado, L. M., Bellouin, N., Sitch, S., Boucher, O., Huntingford, C., Wild, M., & Cox, P. M. (2009). Impacts of changes in diffuse radiation on the global land carbon sink. *Nature*, *458*, 1014–1087.

Miglietta, M. M., Huld, T., & Monforti-Ferrario, F. (2017). Local complementarity of wind and solar energy resources over Europe: An assessment study from a meteorological perspective. *Journal of Applied Meteorology and Climatology*, *56*, 217–234. https://doi.org/10.1175/JAMC-D-16-0031.1

Müller, R., Pfeifroth, U., Traeger-Chatterjee, C., Trentmann, J., & Cremer, R. (2015). Digging the METEOSAT Treasure-3 decades of solar surface radiation. *Remote Sensing*, *7*(6), 8067–8101. https://doi.org/10.3390/rs70608067

Müller, R., Pfeifroth, U., & Traeger-Chatterjee, C. (2015). Towards optimal aerosol information for the retrieval of solar surface radiation using Heliosat. *Atmosphere*, *6*, 863–878. https://doi.org/10.3390/atmos6070863

Mateos, D., Sanchez-Lorenzo, A., Antón, M., Cachorro, V. E., Calbó, J., Costa, M. J., … Wild, M. (2014). Quantifying the respective roles of aerosols and clouds in the strong brightening since the early 2000s over the Iberian Peninsula. *Journal of Geophysical Research: Atmospheres*, *119*, 10,382–10,393. https://doi.org/10.1002/2014JD022076

Nabat, P., Somot, S., Mallet, M., Sanchez-Lorenzo, A., & Wild, M. (2014). Contribution of anthropogenic sulfate aerosols to the changing Euro-Mediterranean climate since 1980. *Geophysical Research Letters*, *15*, 5605–5611. https://doi.org/10.1002/2014GL060798

Norris, J. R., & Wild, M. (2014). Trends in aerosol radiative effects over Europe inferred from observed cloud cover, solar dimming, and solar brightening. *Journal of Geophysical Research: Atmospheres*, *112*, D08214. https://doi.org/10.1029/2006JD007794

Ohmura, A., Dutton, E. G., Forgan, B., Frohlich, C., Gilgen, H., Hegner, H., … Wild, M. (1998). Baseline Surface Radiation Network (BSRN/WCRP): New precision radiometry for climate research,. *Bulletin of the American Meteorological Society*, *79*, 2115–2136. https://doi.org/10.1175/1520-0477(1998)079<2115:BSRNBW>2.0.CO;2

Ohmura, A., & Gilgen, H. (1993). Re-evaluation of the global energy balance. In G. A. McBean, & M. Hantel (Eds.), *Interactions between global climate subsystems the legacy of Hann*. Washington, DC: American Geophysical Union. https://doi.org/10.1029/GM075p0093

Parding, K. M., Liepert, B. G., Hinkelmann, L. M., Ackerman, T. P., Dagestad, K.-F., & Olseth, J. A. (2016). Influence of synoptic weather patterns on solar irradiance variability in northern Europe. *Journal of Climate*, *29*, 4229–4250. https://doi.org/10.1175/JCLI-D-15-0476.1

Pfeifroth, U., Kothe, S., Müller, R., Trentmann, J., Hollmann, R., Fuchs, P., & Werscheck, M (2017). Surface Radiation Data Set-Heliosat (SARAH)—Edition 2, Satellite Application Facility on Climate Monitoring. https://doi.org/10.5676/EUM_SAF_CM/SARAH/V002

Philipona, R., Behrens, K., & Ruckstuhl, C. (2009). How declining aerosols and rising greenhouse gases forced rapid warming in Europe since the 1980s. *Geophysical Research Letters*, *36*, L02806. https://doi.org/10.1029/2008GL036350

Posselt, R., Müller, R. W., Stöckli, R., & Trentmann, J. (2012). Remote sensing of solar surface radiation for climate monitoring—The CM-SAF retrieval in international comparison. *Remote Sensing of Environment*, *118*, 186–198. https://doi.org/10.1016/j.rse.2011.11.016

Posselt, R., Müller, R., Trentmann, J., Stöckli, R., & Liniger, M. A. (2014). A surface radiation climatology across two Meteosat satellite generations. *Remote Sensing of Environment*, *142*, 103–110. https://doi.org/10.1016/j.rse.2013.11.007

Ramanathan, V., Crutzen, P. J., Kiehl, J. T., & Rosenfeld, D. (2001). Aerosols, climate, and the hydrological cycle. *Science*, *294*(5549), 2119–2124. https://doi.org/10.1126/science.1064034

Raschke, E., Kinne, S., Rossow, W. B., Stackhouse Jr., P. W., & Wild, M. (2016). Comparison of radiative energy flows in observational datasets and climate modeling. *Journal of Applied Meteorology and Climatology*, *55*, 93–117. https://doi.org/10.1175/JAMC-D-14-0281.1

Riihelä, A., Carlund, T., Trentmann, J., Müller, R., & Lindfors, A. (2015). Validation of CM SAF surface solar radiation datasets over Finland and Sweden. *Remote Sensing*, *7*(6), 6663–6682. https://doi.org/10.3390/rs70606663

Ruckstuhl, C., & Norris, J. R. (2009). How do aerosol histories affect solar "dimming" and "brightening" over Europe?: IPCC-AR4 models versus observations. *Journal of Geophysical Research*, *114*, D00D04. https://doi.org/10.1029/2008JD011066

Ruckstuhl, C., Philipona, R., Behrens, K., Collaud Coen, M., Dürr, B., Heimo, A., … Zelenka, A. (2008). Aerosol and cloud effects on solar brightening and the recent rapid warming. *Geophysical Research Letters*, *35*, L12708. https://doi.org/10.1029/2008GL034228

Sanchez-Lorenzo, A., Calbó, J., & Wild, M. (2013). Global and diffuse solar radiation in Spain: Building a homogeneous dataset and assessing their trends. *Global and Planetary Change*, *100*(18), 343–352. https://doi.org/10.1016/j.gloplacha.2012.11.010

Sanchez-Lorenzo, A., Enriquez-Alonso, A., Calbó, J., González, J.-A., Wild, M., Follini, D., … Vincente-Serrano, S. M. (2017). Fewer clouds in the Mediterranean: Consistency of observations and climate simulations. *Scientific Reports*, *7*, 41475. https://doi.org/10.1038/srep41475

Sanchez-Lorenzo, A., Enriquez-Alonso, A., Wild, M., Trentmann, J., Vincente-Serrano, S. M., Sanchez-Romero, A., … Hakuba, M. (2017). Trends in downward surface solar radiation from satellites and ground observations over Europe during 1983–2010. *Remote Sensing of the Environment*, *189*, 108–117. https://doi.org/10.1016/j.rse.2016.11.018

Sanchez-Romero, A., Sanchez-Lorenzo, A., Gonzáles, J. A., & Calbó, J. (2016). Reconstruction of long-term aerosol optical depth series with sunshine duration records. *Geophysical Research Letters*, *43*, 1296–1305. https://doi.org/10.1002/2015GL067543

Sanchez-Lorenzo, A., & Wild, M. (2012). Decadal variations in estimated surface solar radiation over Switzerland since the late 19th century. *Atmospheric Chemistry and Physics*, *12*, 8635–8644. https://doi.org/10.5194/acp-12-8635-2012

Sanchez-Lorenzo, A., Wild, M., Brunetti, M., Guijarro, J. A., Hakuba, M. Z., Calbó, J., … Bartók, B. (2015). Reassessment and update of long-term trends in downward surface shortwave radiation over Europe (1939–2012). *Journal of Geophysical Research: Atmospheres*, *120*, 2169–8996. https://doi.org/10.1002/2015JD023321

Schulz, J., Albert, P., Behr, H.-D., Caprion, D., Deneke, H., Dewitte, S., … Zelenka, A. (2009). Operational climate monitoring from space: The EUMETSAT Satellite Application Facility on Climate Monitoring (CM-SAF). *Atmospheric Chemistry and Physics*, *9*, 1687–1709.

Stanhill, G., & Cohen, S. (2001). Global Dimming: A review of the evidence for a widespread and significant reduction in global radiation with discussion of its probable causes and possible agricultural consequences. *Agricultural and Forest Meteorology*, *107*, 255–278. https://doi.org/10.1016/S0168-1923(00)00241-0

Stjern, C. W., Kristjánsson, J. E., & Hansen, A. W. (2009). Global dimming and global brightening—An analysis of surface radiation and cloud cover data in northern Europe. *International Journal of Climatology*, *29*(5), 643–653. https://doi.org/10.1002/joc.1735

Urraca, R, Gracia-Amillo, A. M., Koubli, E., Huld, T., Trentmann, J., Riihelä, A., … Antonanzas-Torres, F. (2017). Extensive validation of CMSAF surface radiation products over Europe. *Remote Sensing of the Environment*, *199*, 171–186. https://doi.org/10.1016/j.rse.2017.07.013

Wild, M. (2009). Global dimming and brightening: A review. *Journal of Geophysical Research*, *114*, D00D16. https://doi.org/10.1029/2008JD011470

Wild, M. (2012). Enlightening global dimming and brightening. *Bulletin of the American Meteorological Society*, *93*(1), 27–37. https://doi.org/10.1175/BAMS-D-11-00074.1

Wild, M. (2016). Decadal changes in radiative fluxes at land and ocean surfaces and their relevance for global warming. *Wiley Interdisciplinary Reviews: Climate Change*, *7*(1), 91–107. https://doi.org/10.1002/wcc.372

Wild, M., Folini, D., Hakuba, M. Z., Schär, C., Seneviratne, S. I., Kato, S., … König-Langlo, G. (2015). The energy balance over land and oceans: An assessment based on direct observations and CMIP5 climate models. *Climate Dynamics*, *44*(11–12), 3393–3429.

Wild, M., Folini, D., Henschel, F., Fischer, N., & Müller, B. (2015). Projections of long-term changes in solar radiation based on CMIP5 climate models and their influence on energy yields of photovoltaic systems. *Solar Energy*, *116*, 12–24. https://doi.org/10.1016/j.solener.2015.03.039

Wild, M., Gilgen, H., Roesch, A., Ohmura, A., Long, C. N., Dutton, E. G., … Tsvetkov, A. (2005). From dimming to brightening: Decadal changes in solar radiation at Earth's surface. *Science*, *308*, 847–850. https://doi.org/10.1126/science.1103215

Wild, M., Ohmura, A., Schär, C., Müller, G., Folini, D., Schwarz, M., … Sanchez-Lorenzo, A. (2017). The Global Energy Balance Archive (GEBA) version 2017: A database for worldwide measured surface energy fluxes. *Earth System Science Data*, *9*, 601–613. https://doi.org/10.5194/essd-9-601-2017

Zák, M., Miksovský, J., & Pišoft, P. (2015). CMSAF radiation data: New possibilities for climatological applications in the Czech Republic. *Remote Sensing*, *7*(11), 14,445–14,457. https://doi.org/10.3390/rs71114445

Zhang, X., Liang, S., Wild, M., & Jiang, B. (2015). Analysis of surface incident shortwave radiation from four satellite products. *Remote Sensing of the Environment*, *165*, 186–202. https://doi.org/10.1016/j.rse.2015.05.015

Zubler, E. M., Folini, D., Lohmann, U., Lthi, D., Schär, C., & Wild, M. (2011). Simulation of dimming and brightening in Europe from 1958 to 2001 using a regional climate model. *Journal of Geophysical Research*, *116*, D18205. https://doi.org/10.1029/2010JD015396